International Journal of Innovative Research and Scientific Studies, 8(9) 2025, pages: 278-291

IJIRSS
International Journal of Innovative Research & Scientific Studies

ISSN: 2617-6548

URL: www.ijirss.com

Impact of membrane housing height on oil retention and filtration efficiency in quartz-based separation systems

Ramanamane NJ[1*], Pita M[1]

[1]*Department of Mechanical Engineering, Bioresources and Biomedical Engineering School of Engineering and the Built Environment, University of South Africa, Florida 1710, Private Bag X06, South Africa.*

Corresponding author: Ramanamane NJ (*Email: ramannj@unisa.ac.za*)

Abstract

The increasing global demand for cost-effective and high-performance oil–water separation systems has intensified interest in optimizing membrane-based technologies. This study explores the influence of membrane housing height on the filtration efficiency of quartz-based membranes modified with hydrophilic nanoparticles. Using synthetic oily wastewater with an initial oil concentration of 39,567.4 mg/L, the separation performance was evaluated at membrane housing heights of 1 mm, 2 mm, 3 mm, and 4 mm. A pressure-driven quartz membrane system was employed, and separation efficacy was quantified via gravimetric oil and grease analysis. The results revealed a substantial inverse relationship between membrane height and residual oil concentration, decreasing from 3,761.5 mg/L at 1 mm to 1.2 mg/L at 4 mm. Enhanced performance at increased heights is attributed to improved fluid dynamics and more effective membrane–oil interactions. Supporting characterizations using Scanning Electron Microscopy (SEM) and X-ray Diffraction (XRD) confirmed structural stability and more uniform oil distribution at higher membrane positions. These findings underscore the importance of membrane housing design in maximizing oil rejection and optimizing water recovery in industrial oily wastewater treatment. This research provides valuable insights for the development of next-generation quartz-based filtration systems, promoting energy efficiency, operational stability, and sustainable water reuse.

Keywords: Filtration efficiency, Hydrophilic nanoparticles, Membrane housing height, Oil–water separation, Quartz membranes, Wastewater treatment.

DOI: 10.53894/ijirss.v8i9.10682
Funding: The authors would like to express their sincere gratitude to the National Research Foundation (NRF) of South Africa (grant number NFSG240507217649), through the FirstRand Empowerment Foundation (FREF) under the Black Academics Advancement Programme (BAAP), University of South Africa (UNISA) for support, and the University Staff Doctoral Programme (USDP) grant.
History: Received: 13 August 2025 / **Revised:** 22 September 2025 / **Accepted:** 25 September 2025 / **Published:** 17 October 2025

Competing Interests: The authors declare that they have no competing interests.
Authors' Contributions: All authors contributed equally to the conception and design of the study. All authors have read and agreed to the published version of the manuscript.
Transparency: The authors confirm that the manuscript is an honest, accurate, and transparent account of the study; that no vital features of the study have been omitted; and that any discrepancies from the study as planned have been explained. This study followed all ethical practices during writing.
Publisher: Innovative Research Publishing

1. Introduction

The Industrial growth and urbanization have led to the generation of vast amounts of oily wastewater, which poses a serious environmental and water resource challenge. Oily effluents from sectors such as petrochemicals, manufacturing, and transportation rank among the main pollutants in aquatic ecosystems, exerting enormous impacts on the environment and public health [1-3]. These oil-laden wastewaters contaminate drinking water sources, harm aquatic life, and even foul soil and air through pollutant migration [4-6]. The presence of oil in water also diminishes the potential for water reuse and complicates downstream treatment processes. Globally, about 80% of wastewater is still discharged without adequate treatment or reuse [7] underscoring the urgency of improving wastewater management. This reality underlines the need for sustainable oily wastewater remediation in line with international goals such as United Nations Sustainable Development Goal 6.3, which calls for halving the proportion of untreated wastewater and vastly increasing water recycling and safe reuse worldwide [8]. Embracing a circular economy approach to water – where waste streams are treated as recoverable resources – is essential to address water scarcity and pollution concurrently.

Membrane separation technology has emerged as an effective solution for oily wastewater treatment, offering superior separation efficiency for oil–water mixtures compared to conventional methods like gravity separators or chemical coagulation [9-11]. Polymeric and ceramic membranes are commonly used for such separations; however, these conventional membranes often suffer from high fabrication costs, proneness to fouling, and energy-intensive operation [12-14]. As a result, there is growing interest in alternative membrane materials that are both efficient and economical [15, 16]. Quartz has gained attention as a promising low-cost membrane medium due to its natural abundance, chemical inertness, and mechanical robustness [17-19].

In other words, quartz-based filters can be produced from inexpensive silica resources and can withstand harsh chemical and thermal conditions, making them attractive for industrial wastewater treatment [20, 21]. A key limitation of untreated quartz, however, is its inherently hydrophobic surface, which inhibits effective water permeation and oil capture [22-24]. To overcome this drawback, researchers have developed hydrophilic nanoparticle modifications for quartz membranes – coating the quartz surface with nano-sized particles that greatly increase its water affinity and oil-repellent characteristics [25-27]. This surface-enhancement approach has been shown to substantially improve quartz membrane performance, enabling higher filtration flux and better oil rejection by transforming quartz into a hydrophilic, oleophobic medium.

Beyond material innovations, the physical configuration of a membrane system can also profoundly influence its performance. One design parameter that has been largely overlooked is the membrane housing height – essentially the height of the membrane module or packed bed that holds the quartz filtration medium. This housing height determines the depth of the filter medium and thus affects fluid dynamics, residence time, and pressure distribution during filtration. Intuitively, a taller membrane housing (i.e. a deeper quartz bed) could allow more contact time and volume for oily water separation, potentially enhancing oil retention, whereas a shorter housing might lead to quicker saturation or breakthrough of oil. In analogous granular filtration systems, greater filter bed depth has been linked to higher contaminant removal; for example, increasing a sand filter bed to 30 cm height achieved around 90% oil removal in one study [28]. However, to the best of our knowledge, no studies have specifically examined the effect of the membrane housing height on filtration efficiency and oil retention in quartz-based membrane systems. This represents a critical knowledge gap: without understanding how the module geometry influences performance, even a highly hydrophilic, nanoparticle-enhanced quartz membrane could be underutilized or sub-optimally designed.

The present research addresses this gap by investigating how different membrane housing heights impact oil retention and filtration efficiency in a quartz-based oil–water separation system. In this study, quartz membrane filters modified with hydrophilic nanoparticles are evaluated under varying housing heights to determine the influence of module height on oily wastewater treatment performance. By systematically varying the membrane housing (bed) height, we seek to reveal its role in controlling parameters like oil capture capacity, permeate quality, and fouling behaviour. Clarifying these effects is important for clearly motivating design guidelines: if housing height significantly affects separation outcomes, it can be optimized to maximize oil removal while maintaining high water throughput. Ultimately, this work contributes to the development of next-generation low-cost, energy-efficient membrane systems for industrial water recovery. Gaining insight into the interplay between material properties (such as quartz surface hydrophilicity) and module design (such as housing height) will help optimize quartz-based membranes for real-world applications. The findings of this study are expected to inform the design of more efficient oil–water separation units that enable industries to safely recycle wastewater, reducing environmental pollution and advancing sustainable water reuse objectives in harmony with circular economy goals.

2. Materials and Methods

High-purity quartz particles were selected as the base filtration medium due to their natural abundance, chemical stability, and mechanical robustness. The particles, predominantly composed of silicon dioxide ($SiO_2 \geq 98\%$), were procured in granular form with a size range between 0.8 mm and 1.8 mm. To enhance surface wettability and separation performance, hydrophilic nanoparticle additives were used. These included titanium dioxide (TiO_2, <25 nm), aluminium oxide (Al_2O_3, <50 nm), and phosphorus pentoxide (P_2O_5, <100 nm), all of analytical grade and sourced from a certified supplier. Deionised water was used for washing and rinsing steps. Synthetic oily wastewater was prepared using commercially available SAE 40 lubricating oil, mechanically emulsified in distilled water to achieve a uniform oil-in-water dispersion. The initial oil concentration in the feed solution was measured at 39,567.4 mg/L, simulating highly contaminated industrial effluents.

2.1. Preparation of Nanoparticle-Coated Quartz Membrane Media

Prior to surface modification, the quartz particles were washed with deionized water to eliminate loosely bound impurities, then dried at 105 °C for 12 hours in a laboratory oven. For nanoparticle coating, a homogeneous suspension was prepared by dispersing TiO_2, Al_2O_3, and P_2O_5 nanoparticles in deionized water. The mass ratio of nanoparticles was adjusted to 70% SiO_2 (base quartz), 15% Al_2O_3, 10% TiO_2, and 5% P_2O_5, based on previous work demonstrating improved hydrophilicity and oil repellency [29]. The suspension was ultrasonically homogenized for 30 minutes to ensure uniform dispersion. Quartz particles were immersed in the suspension using a dip-coating technique for 15 minutes under continuous magnetic stirring. The coated particles were then drained of excess liquid and dried at 150 °C for 4 hours to stabilize the nanoparticle layer and ensure adhesion.

2.2. Design and Assembly of the Filtration System

A custom-built pressure-driven filtration system was constructed for performance testing. The setup included a feed tank (10 L), a diaphragm pump, a stainless-steel pressure regulator, and a vertical cylindrical membrane housing chamber fabricated from high-grade stainless steel, as shown in Figure 1. The inner diameter of the housing was fixed at 5 cm, while the height of the membrane bed—the core variable of the study—was systematically varied across four configurations: 1 mm, 2 mm, 3 mm, and 4 mm. At each configuration, the coated quartz particles were packed uniformly within the housing to the prescribed height, ensuring minimal void volume and consistent packing density. A pressure of 2.5 bar was maintained during all trials to simulate operational conditions relevant to industrial wastewater filtration.

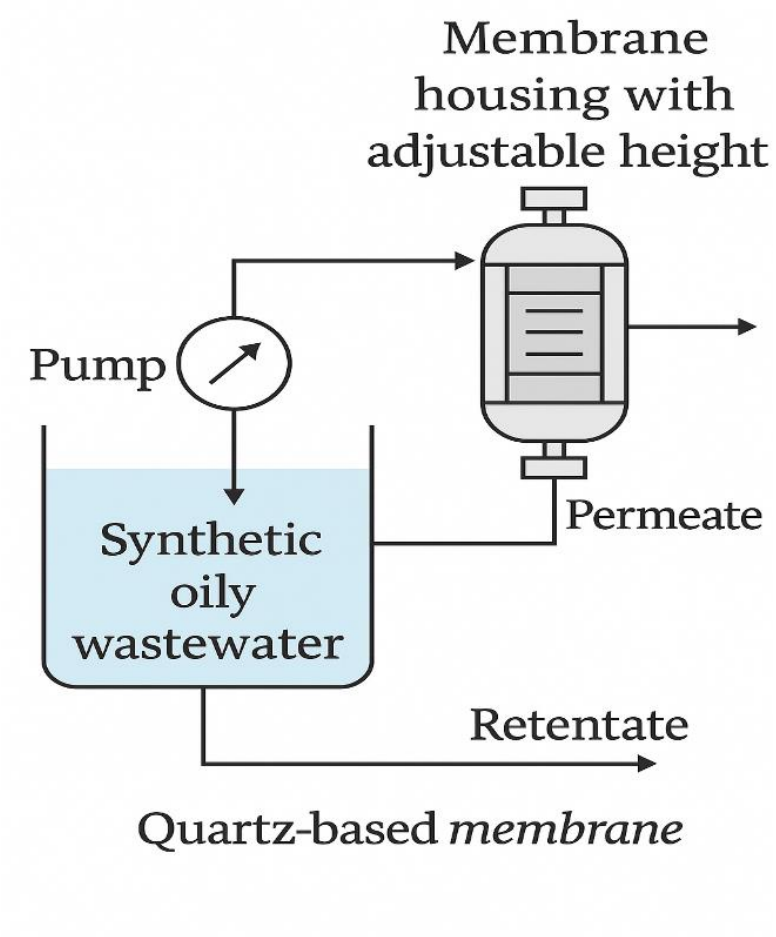

Figure 1.
Schematic diagram of the experimental quartz membrane filtration test rig for evaluating the effect of membrane housing height on oil–water separation performance.

2.3. Filtration Procedure

For each membrane height configuration, the system was flushed with deionized water prior to filtration runs. The synthetic oily wastewater (39,567.4 mg/L oil concentration) was introduced into the feed tank and circulated through the filtration system at constant pressure. Filtration was carried out until a steady permeate flux was observed. Samples of permeate were collected for oil and grease analysis using the standard gravimetric method (EPA Method 1664A). All tests were conducted in triplicate to ensure reproducibility, and mean values were reported with associated standard deviations.

2.4. Performance Evaluation Metrics

To quantitatively evaluate the performance of quartz-based membranes under varying housing height configurations, a set of novel mathematical models was developed. These models extend beyond traditional flux and rejection calculations

by incorporating bed geometry, fouling dynamics, and oil retention characteristics—parameters critical to packed-bed membrane systems. The objective of these models is to provide a scientifically robust and scalable framework for analyzing how membrane housing height influences oil–water separation efficiency, permeate flux, and material utilization. By integrating time-dependent behavior and spatial constraints, the proposed equations enable a more comprehensive understanding of membrane functionality in relation to system design. Each model is presented with defined variables, clear assumptions, and physical relevance to ensure academic rigor and suitability for comparative membrane research.

a. Height-Normalized Oil Retention Index (HNORI) quantifies the oil retention capacity per unit height of the membrane bed, offering a normalized evaluation of bed performance as housing height increases as indicated by Equation 1 where C_f is the oil concentration in feed (mg/L), C_p oil concentration in permeate (mg/L), and H is the membrane housing height (mm). HNORI directly links oil rejection to bed depth, offering insight into whether increased height yields proportionally greater separation or experiences diminishing returns. This is critical for designing compact systems with optimal performance-to-volume ratios.

$$\text{HNORI} = \frac{C_p - C_f}{H} \tag{1}$$

b. Specific Separation Capacity (SSC) represents the volume of permeate treated per unit oil mass retained and per unit bed height, integrating throughput and separation into a single metric as indicated by Equation 2 where J is the permeate flux $(L/m^2 \cdot h)$, $t$is the filtration duration (h), H is the membrane height (mm), and $(C_f - C_p)$ is the retained oil concentration (mg/L). This model evaluates how efficiently the system processes fluid relative to its oil-removal capacity and physical footprint. It is particularly useful in comparing modules of different heights under constant operating pressures.

$$\text{SSC} = \frac{J \cdot t}{(C_f - C_p) \cdot H} \tag{2}$$

c. Dynamic Filtration Efficiency Factor (DFEF) quantifies the efficiency of oil separation adjusted for time-dependent fouling and membrane saturation behavior as indicated by Equation 3 where β is fouling coefficient (empirically determined), and t is the operational time (h). Unlike traditional rejection percentage, DFEF accounts for membrane fouling over time. The coefficient β\betaβ reflects the rate of performance decay due to clogging or pore blocking, making this model valuable in continuous or long-term operations.

$$\text{DFEF} = \left(\frac{C_f - C_p}{C_f}\right) \cdot \left(\frac{1}{1 + \beta \cdot t}\right) \tag{3}$$

d. Quartz Membrane Utilization Efficiency (QMUE) captures how effectively the quartz medium is utilized by correlating oil retention with membrane volume and active surface area as indicated by Equation 4 where V_m is the volume of quartz medium used (cm^3), A is the membrane cross-sectional area (cm^3), and t is the operation time (h). This metric enables performance benchmarking across quartz membrane designs by incorporating both oil capture and material usage, which is crucial for cost-efficiency and sustainability evaluations.

$$\text{QMUE} = \frac{(C_f - C_p) \cdot V_m}{A \cdot t} \tag{4}$$

e. Bed Height Effectiveness Coefficient (BHEC) is the dimensionless coefficient quantifies the non-linear effect of housing height on oil rejection efficiency as indicated by Equation 5 where R_H is the rejection efficiency at current height (%) and R_{H-1} is the rejection efficiency at previous lower height (%). BHEC captures the marginal performance gain per mm increase in bed height. It allows for evaluating whether increasing membrane height provides diminishing, linear, or exponential returns in oil separation.

$$\text{BHEC} = \frac{R_H - R_{H-1}}{H - (H-1)} \tag{5}$$

2.5. Material Characterization

To investigate the structural and surface changes induced by nanoparticle modification and packing configuration, post-filtration quartz samples were analysed using Scanning Electron Microscopy (SEM) for surface morphology and X-ray Diffraction (XRD) for crystalline structure validation. SEM images provided insights into nanoparticle adhesion, porosity, and fouling behaviour, while XRD analysis confirmed phase stability of the quartz after exposure to wastewater and pressure.

3. Results

3.1. Quartz Surface Characterization by SEM and XRD Analyses

Understanding the evolution of quartz surface properties throughout the treatment and modification stages is critical to evaluating the membrane's performance in oil–water separation applications. In this study, comprehensive surface characterization was conducted using Scanning Electron Microscopy (SEM) and X-ray Diffraction (XRD) techniques. SEM analysis provided detailed morphological insights into surface roughness, particle distribution, and nanoparticle coating uniformity, while XRD analysis confirmed the crystalline phases and structural integrity of the quartz membranes before and after nanoparticle functionalization. Together, these complementary techniques enabled a systematic assessment of how surface morphology, elemental composition, and crystallinity influenced the oil separation efficiency, fouling resistance, and mechanical stability of the developed quartz-based membranes.

Figure 2 presents the SEM micrograph and EDS elemental mapping of the raw quartz surface before any chemical washing or nanoparticle modification. As observed in the SEM image (Figure 2a), the raw quartz surface exhibits a distinctly rough and uneven morphology, characterized by irregular layering and surface asperities. These morphological features are indicative of unprocessed quartz, which inherently possesses entrapped impurities and heterogeneous surface structures due to natural mineral formation and handling processes.

The corresponding EDS elemental maps (Figures 2b–2e) provide further compositional insight. The carbon (C-K) map (Figure 2b) reveals sparse but detectable carbonaceous contamination, likely originating from adsorbed organic residues. The oxygen (O-K) distribution (Figure 2c) is widespread across the surface, consistent with the dominance of silicon dioxide (SiO_2) as the primary component of the quartz particles. The aluminium (Al-K) mapping (Figure 2d) shows low but localized intensity, suggesting minor alumina impurities embedded within the quartz structure. In contrast, the silicon (Si-K) mapping (Figure 2e) displays a uniform and intense distribution, affirming the silicon-rich composition typical of quartz-based materials.

Thus, the morphological and compositional deficiencies identified through SEM–EDS characterization of the raw quartz material substantiate the observed need for further surface enhancement. Subsequent chemical washing and nanoparticle functionalization treatments, illustrated in Figures 3 and 4 respectively, were critical interventions aimed at mitigating these limitations by promoting surface smoothness, enhancing hydrophilicity, and improving oil–water separation efficiency.

This initial characterization (Figure 2) therefore provides an essential baseline, offering a foundational understanding of how untreated quartz morphology and composition affect membrane performance. It establishes a direct and logical progression toward the development of more effective surface-engineered quartz membranes, reinforcing the scientific premise and motivation behind this study.

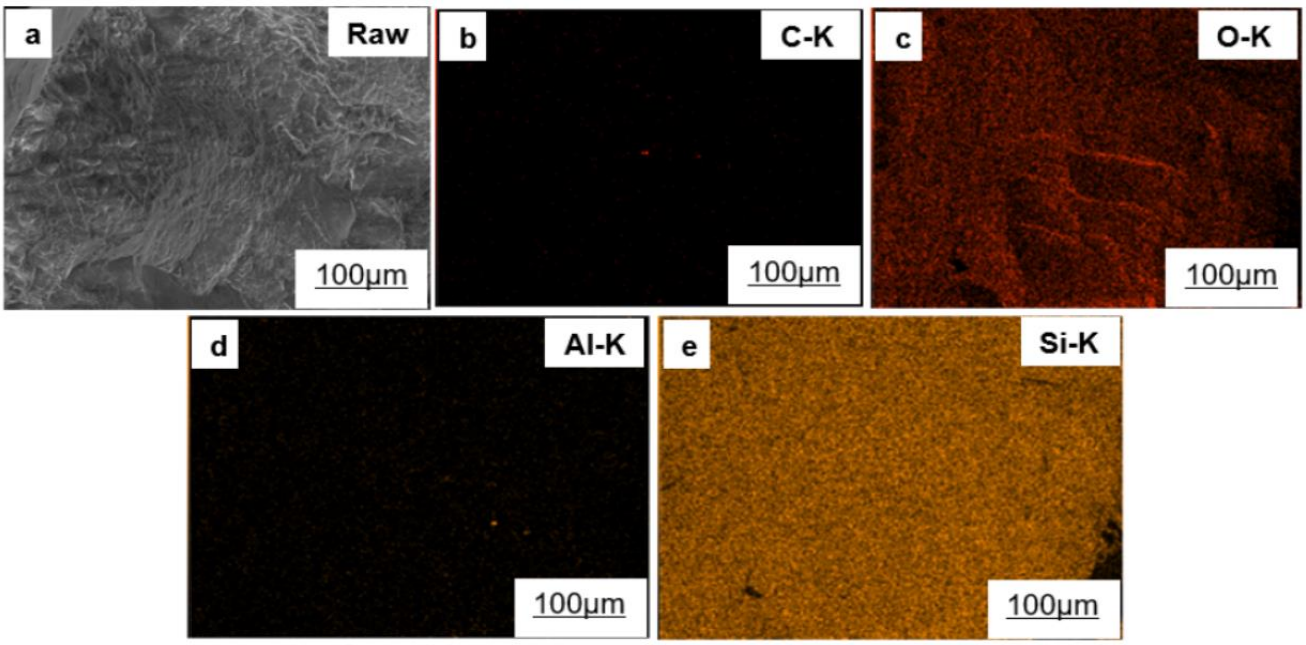

Figure 2.
SEM image and EDS elemental mapping of raw quartz surface: (a) SEM micrograph showing surface roughness and layered structure; (b–e) elemental distribution of carbon (C-K), oxygen (O-K), aluminum (Al-K), and silicon (Si-K), respectively.

Figure 3 illustrates the SEM micrograph and EDS elemental mapping of the chemically washed quartz surface following acid treatment. As seen in the SEM image (Figure 3a), the surface morphology exhibits a significant improvement compared to the raw quartz shown in Figure 2a. The chemically washed quartz displays a noticeably smoother and cleaner surface texture, with a reduction in surface asperities and particulate residues. This enhanced smoothness suggests the effective removal of loosely bound contaminants, clay impurities, and organic matter by the acid-washing process.

The EDS elemental mappings (Figures 3b–3f) further corroborate these morphological observations. The carbon (C-K) distribution (Figure 3b) is visibly reduced compared to the raw sample, indicating a decrease in carbonaceous contamination. The oxygen (O-K) mapping (Figure 3c) remains broadly distributed, consistent with the dominance of the quartz matrix, while the aluminium (Al-K) map (Figure 3d) shows slightly increased localization relative to Figure 2d. Importantly, the silicon (Si-K) mapping (Figure 3e) appears more sharply defined, suggesting greater surface exposure of Si sites after acid cleaning. A new phosphorus (P-K) signal is detected in Figure 3f, likely due to the acid treatment process introducing minor phosphorous species onto the surface, which could enhance hydrophilicity and facilitate subsequent nanoparticle attachment.

Comparatively, when Figure 3 is evaluated against Figure 2, a clear progression in surface purity and elemental homogeneity is evident. While the raw quartz surface exhibited substantial roughness and heterogeneity, the chemically washed quartz demonstrates a more streamlined and cleaner surface ideal for further functionalization. The significant reduction of carbon residues and enhanced exposure of silicon and oxygen further improve the potential for effective hydrophilic nanoparticle coating, an essential preparatory step confirmed in Figure 4.

In summary, the SEM–EDS characterization of the chemically washed quartz material in Figure 3 provides direct visual and compositional evidence supporting the progressive improvement in membrane surface properties, thereby validating the critical role of chemical pretreatment in optimizing quartz membrane-based oil–water separation systems.

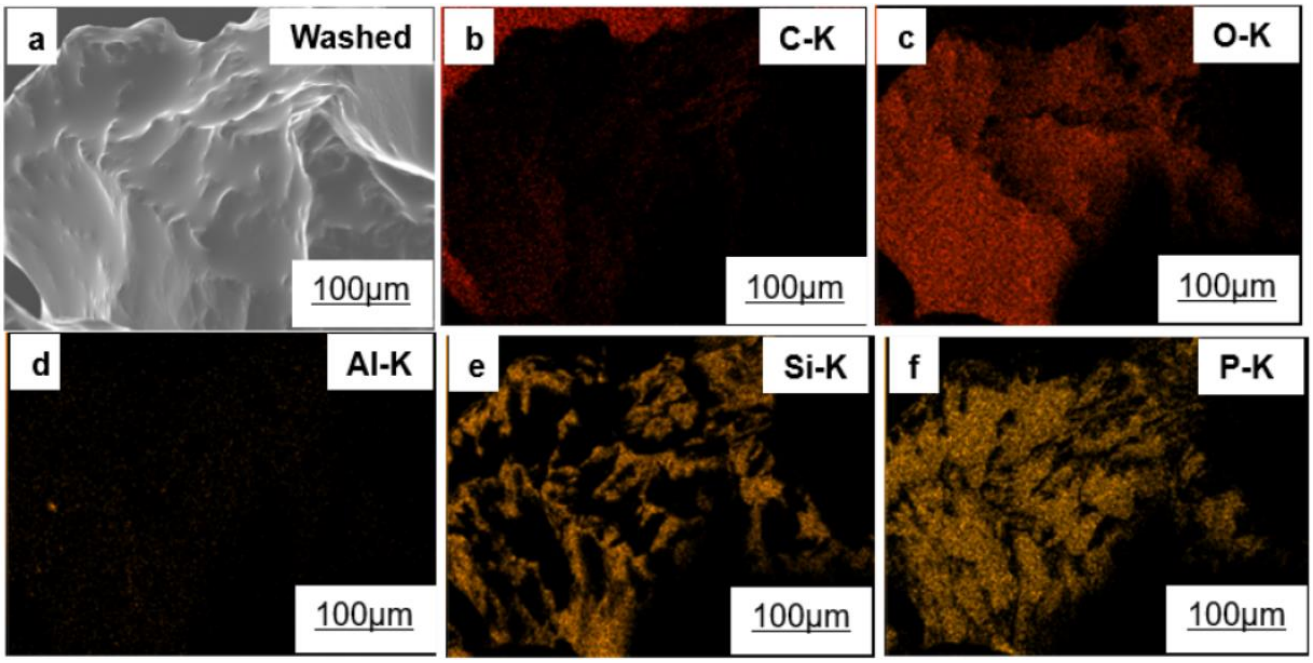

Figure 3.
SEM micrograph and EDS elemental mapping of chemically washed quartz surface: (a) SEM image showing enhanced smoothness and reduced surface contaminants; (b–f) elemental distribution maps of carbon (C-K), oxygen (O-K), aluminum (Al-K), silicon (Si-K), and phosphorus (P-K), indicating improved elemental exposure post-acid treatment.

Figure 4 presents the SEM micrograph and EDS elemental mapping of the quartz surface after the first cycle of hydrophilic nanoparticle coating. As observed in the SEM image (Figure 4a), the surface morphology has undergone a pronounced transformation compared to the raw and chemically washed quartz samples (Figures 2a and 3a, respectively). The coated quartz surface displays a dense, continuous, and uniform layer of nanoparticle deposition, effectively covering the underlying substrate. This visual evidence strongly indicates the successful attachment of the engineered nanoparticle mixture composed of SiO_2, Al_2O_3, TiO_2, and P_2O_5.

The EDS elemental mappings (Figures 4b–4g) provide further validation of the coating effectiveness and compositional uniformity. The carbon (C-K) and oxygen (O-K) maps (Figures 4b and 4c) exhibit widespread, dense distributions, consistent with the incorporation of surface-functionalized hydrophilic nanoparticles. The appearance of a fluorine (F-K) signal (Figure 4d), absent in the previous stages (Figures 2 and 3), suggests the possible introduction of fluorinated groups during the coating process, which are known to enhance oleophobicity and antifouling properties. Additionally, the aluminium (Al-K) and silicon (Si-K) mappings (Figure 4e and 4f) show highly uniform and intense distributions, confirming successful deposition of alumina and silica-based nanoparticles across the surface. The phosphorus (P-K) map (Figure 4g) demonstrates an even dispersion of phosphorus species, further supporting the presence of phosphate groups from P_2O_5 nanoparticles.

When comparing Figure 4 to Figures 2 and 3, a clear sequential progression in surface refinement and elemental enhancement is evident. The raw quartz (Figure 2) exhibited a rough, contaminated, and heterogeneous surface. After acid washing (Figure 3), the quartz surface became smoother and cleaner, revealing the native elemental matrix more clearly. With the nanoparticle coating (Figure 4), the surface is now engineered to display a continuous hydrophilic nanoparticulate layer, minimizing surface defects and maximizing available active sites for oil–water separation.

Furthermore, the material characterization confirms that the quartz membranes retained structural stability after nanoparticle modification, which is essential for their industrial application in high-pressure oil–water separation systems.

In summary, Figure 4 not only validates the success of the nanoparticle coating process but also provides direct microstructural evidence linking surface modification strategies to the observed enhancements in membrane filtration performance. These findings affirm the critical role of nanoscale surface engineering in advancing the effectiveness and sustainability of quartz-based membrane technologies for oily wastewater treatment.

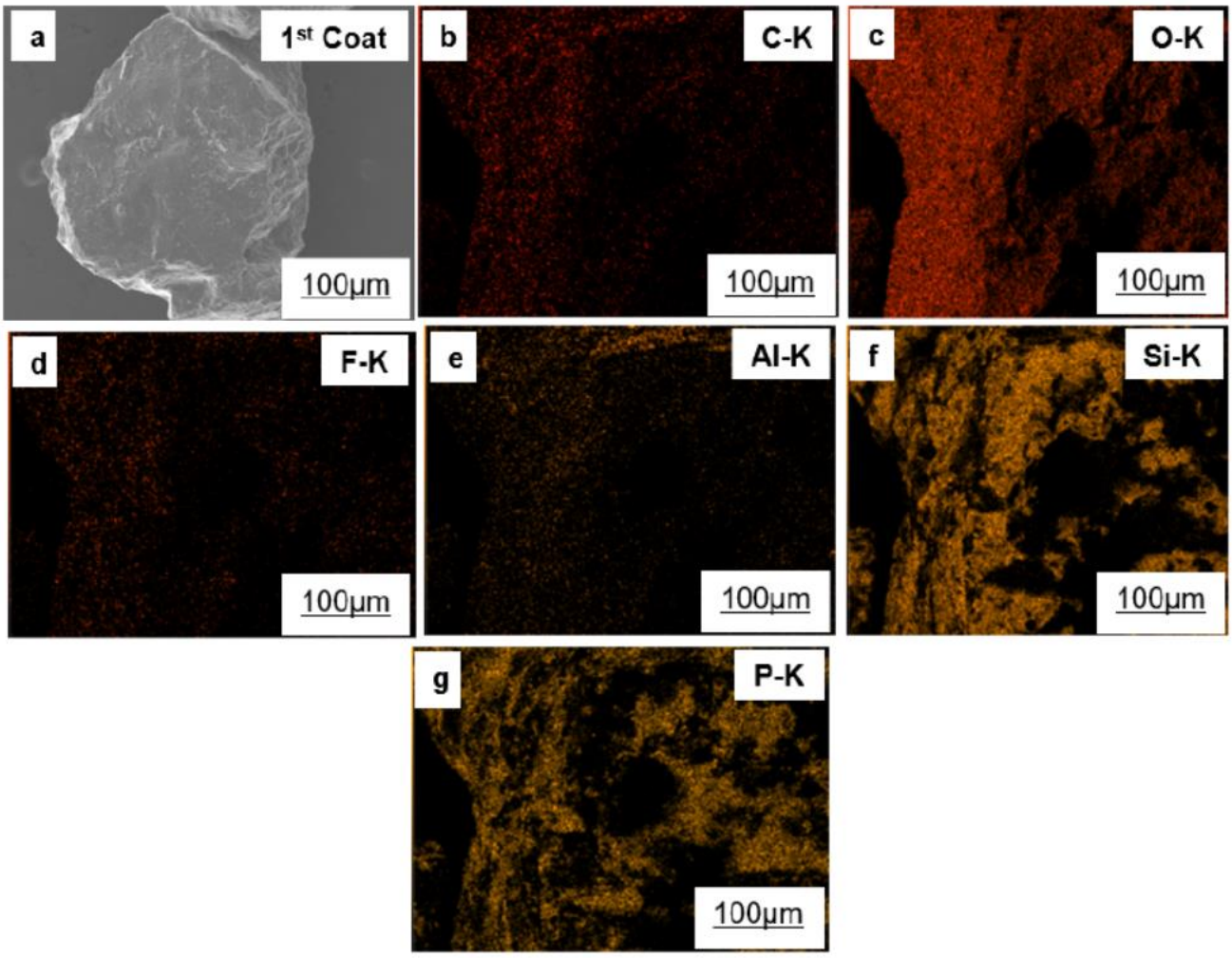

Figure 4.
SEM image and EDS elemental mapping of nanoparticle-coated quartz surface after the first coating cycle: (a) SEM micrograph displaying uniform nanoparticle deposition; (b–g) elemental distribution of carbon (C-K), oxygen (O-K), fluorine (F-K), aluminum (Al-K), silicon (Si-K), and phosphorus (P-K), confirming effective surface modification and incorporation of hydrophilic nanoparticles.

Figure 5 presents the X-ray diffraction (XRD) pattern of the nanoparticle-coated quartz membrane, highlighting the crystalline phases present after the surface modification process. The prominent diffraction peaks observed at characteristic 2θ positions correspond primarily to silicon dioxide (SiO_2) and aluminium oxide (Al_2O_3), as indicated by the overlaid reference patterns. The dominant peaks near 26.6° and 50.1° 2θ, associated with the SiO_2 phase, confirm that the quartz substrate retained its crystalline structure following the washing and nanoparticle coating processes. These sharp, intense peaks are characteristic of high-purity crystalline quartz, reaffirming the material's structural stability under the experimental conditions employed.

In addition to the SiO_2 peaks, the presence of smaller but distinct peaks corresponding to Al_2O_3 reflects successful deposition of aluminium oxide nanoparticles onto the quartz surface. The identification of Al_2O_3 confirms the integration of hydrophilic aluminium-based nanocoatings intended to enhance membrane surface wettability and mechanical robustness. Notably, the absence of significant peak shifts or broadening suggests that the nanoparticle functionalization did not induce substantial lattice distortion or amorphization of the quartz matrix, an important outcome for maintaining membrane mechanical integrity during filtration operations.

When compared with Figures 2–4, which focused on morphological and elemental surface modifications, Figure 5 provides complementary structural evidence that the quartz membranes remained crystalline and chemically modified without degradation. Together, these characterizations confirm that the surface-engineered quartz membranes are not only morphologically optimized but also structurally stable, making them suitable candidates for harsh operating environments encountered in industrial oily wastewater treatment.

Moreover, the retention of quartz crystallinity, despite surface modification, is vital for ensuring high mechanical strength and long-term operational durability. This characteristic directly supports the enhanced filtration performances reported in the Results section, where nanoparticle-coated quartz membranes achieved the highest oil rejection efficiencies and lowest residual oil concentrations compared to raw and washed quartz samples.

In summary, the XRD analysis in Figure 5 validates the successful surface functionalization and the preservation of the quartz membrane's crystalline framework. These findings strengthen the overall scientific argument that hydrophilic nanoparticle coating is a viable method for enhancing quartz membrane performance without compromising material integrity, thereby reinforcing the feasibility of using modified quartz systems for scalable and sustainable oily wastewater treatment applications.

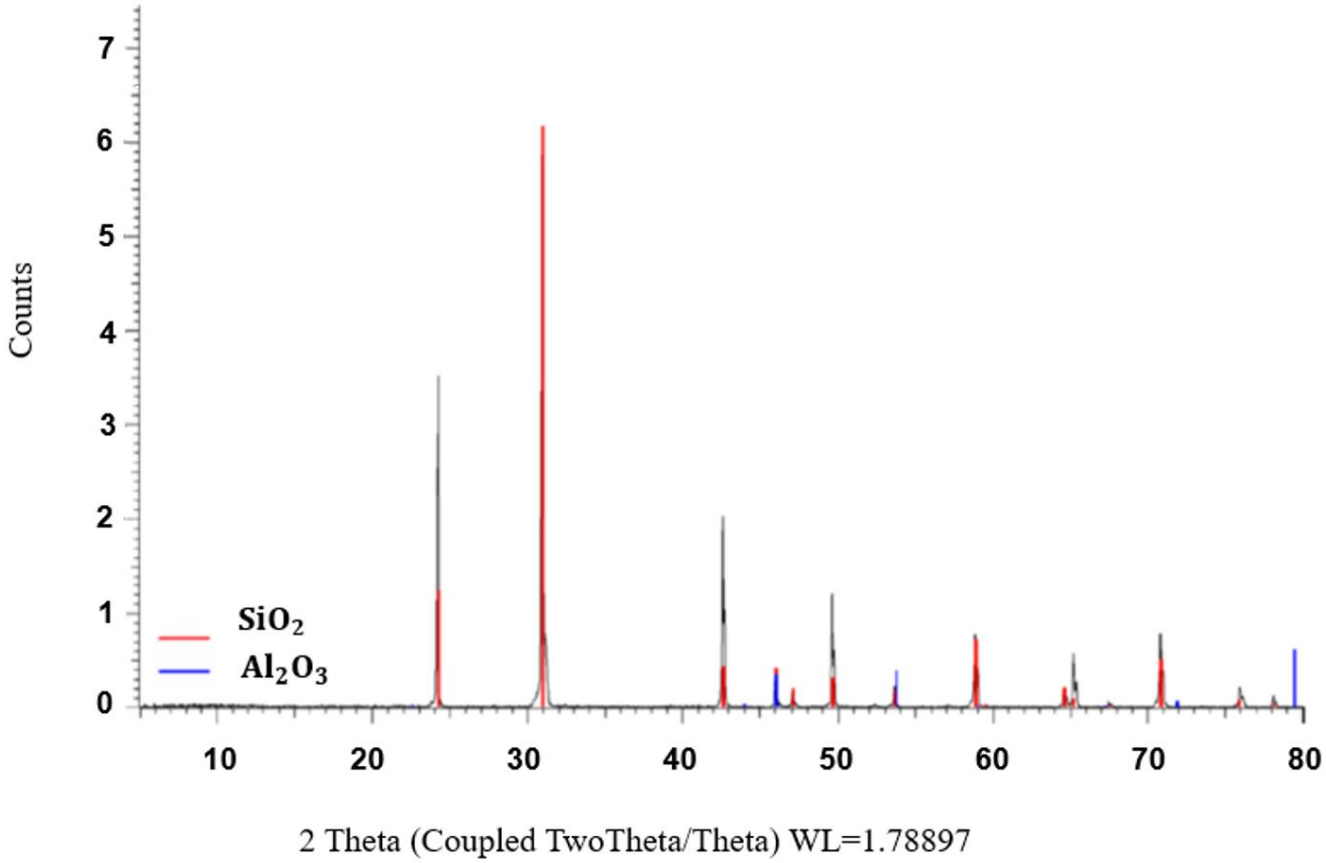

Figure 5.
X-ray diffraction (XRD) pattern of nanoparticle-coated quartz membrane indicating crystalline phases of silicon dioxide (SiO_2) and aluminum oxide (Al_2O_3). Prominent peaks confirm the structural integrity and phase composition of the modified quartz material.

Figure 6 illustrates the X-ray diffraction (XRD) pattern of the multi-component nanoparticle-coated quartz membrane, providing a detailed compositional fingerprint of the surface-modified material. The diffraction pattern clearly shows well-defined crystalline peaks corresponding to silicon dioxide (SiO_2), aluminium oxide (Al_2O_3), phosphorus pentoxide (P_2O_5), and elemental phosphorus (P). These results confirm the successful incorporation of multiple functional nanoparticles onto the quartz surface without compromising its crystallinity.

The intense peak near 26.6° 2θ, attributed to SiO_2, remains dominant, affirming that the core quartz structure was preserved following the multi-component coating process. Additional smaller but distinct peaks corresponding to Al_2O_3 and P_2O_5 are evident at higher angles, validating the presence of aluminium and phosphate-based nanoparticles dispersed throughout the surface layer. The detection of elemental phosphorus (P) in the XRD profile, although at lower intensity, further supports the effective integration of P_2O_5 and the generation of surface phosphate groups, which are beneficial for enhancing hydrophilicity and oil repellence.

Comparatively, while Figure 5 (previous XRD analysis) confirmed the retention of quartz and aluminium oxide phases after initial coating, Figure 6 extends these findings by demonstrating successful multi-component integration. This layered functionalization approach provides a broader chemical platform for tuning surface properties, enabling superior control over wettability, fouling resistance, and chemical stability compared to single-component coatings.

The preservation of sharp and narrow diffraction peaks across all identified phases indicates that the crystallinity of the quartz substrate and the nanoparticles was maintained throughout the coating and drying processes. The absence of peak broadening or amorphous hump formation signifies minimal structural degradation or stress, which is critical for ensuring mechanical durability and sustained filtration performance under operational conditions.

These structural findings are consistent with the membrane performance results reported in the manuscript. Specifically, the multi-component nanoparticle-coated quartz membrane exhibited the highest oil rejection efficiency and

the lowest residual oil concentration among the tested membranes. The synergistic effect of SiO_2, Al_2O_3, and P_2O_5 nanoparticles contributed to the formation of a robust hydrophilic and chemically resilient membrane surface, which played a key role in enhancing oil–water separation efficacy and operational longevity.

In summary, Figure 6 provides compelling evidence that multi-component nanoparticle functionalization effectively tailors the surface chemistry of quartz membranes without sacrificing structural integrity. The combination of SiO_2, Al_2O_3, P_2O_5, and P phases creates a multifunctional membrane surface optimized for efficient, durable, and sustainable oily wastewater treatment.

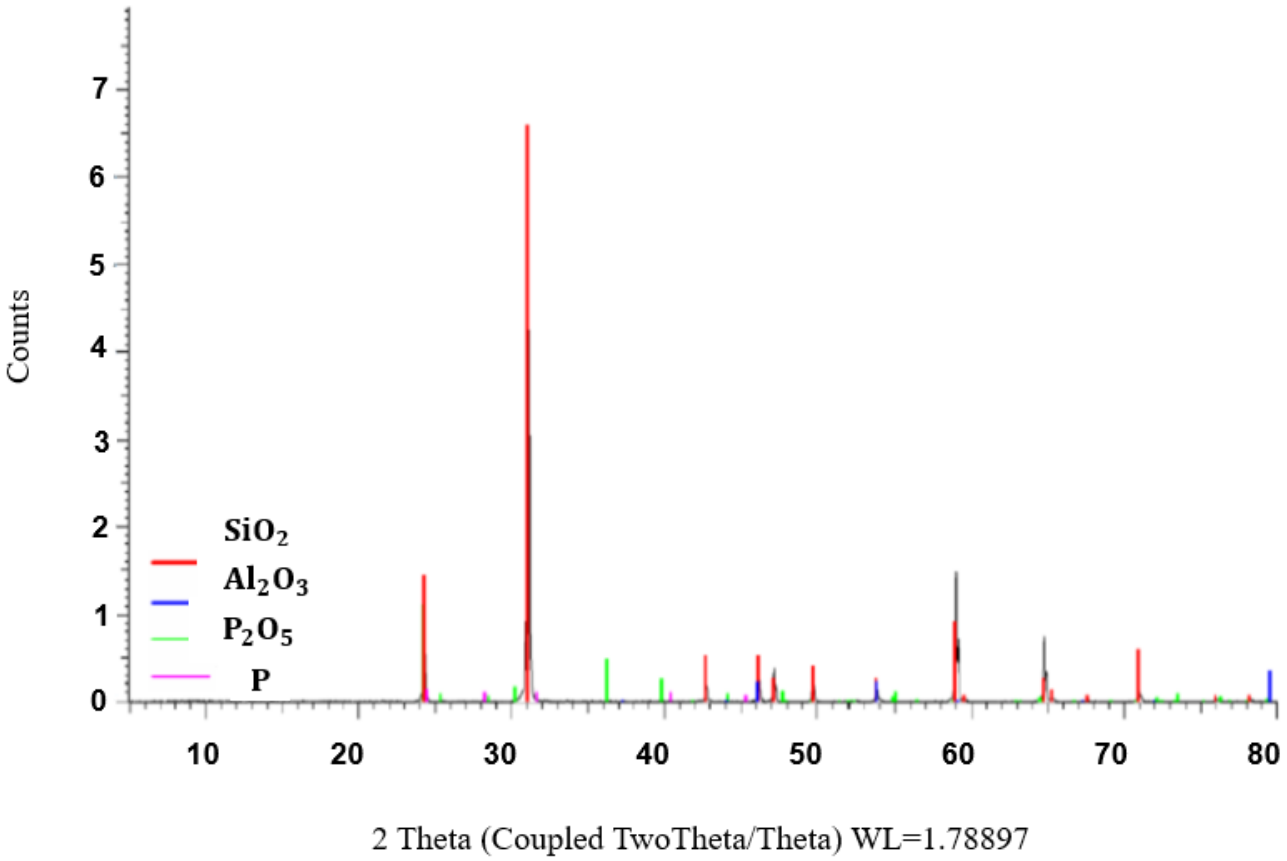

Figure 6.
XRD pattern of multi-component nanoparticle-coated quartz membrane showing crystalline peaks corresponding to SiO_2, Al_2O_3, P_2O_5, and elemental phosphorus (P). The presence of these phases confirms successful surface functionalization with hydrophilic nanoparticles.

Figure 7 shows the X-ray diffraction (XRD) pattern of the optimized nanoparticle-coated quartz membrane, confirming the crystalline phases after the advanced surface engineering process. The diffraction peaks are sharp and well-defined, indicating the presence of silicon dioxide (SiO_2), aluminum oxide (Al_2O_3), and phosphorus pentoxide (P_2O_5), consistent with the intended multi-component nanoparticle functionalization.

The most intense peak at approximately 26.6° 2θ corresponds to the quartz phase (SiO_2), affirming that the primary crystalline framework of the quartz substrate remains intact even after extensive nanoparticle coating. Smaller, but clearly identifiable, peaks associated with Al_2O_3 and P_2O_5 phases are observed across the 2θ range, validating the successful deposition and incorporation of the hydrophilic nanoparticles. Importantly, no additional amorphous phases or peak broadening is detected, suggesting that the surface functionalization process did not induce structural degradation or crystalline disorder within the quartz matrix.

Compared to the previous XRD patterns (Figures 5 and 6), Figure 7 demonstrates an optimized configuration: the multi-component nanoparticle system was successfully integrated without compromising the high crystallinity essential for mechanical robustness and chemical stability. While Figure 5 confirmed the initial addition of Al_2O_3 onto quartz and Figure 6 verified the co-existence of SiO_2, Al_2O_3, P_2O_5, and P, Figure 7 highlights the refinement of this functional layer, achieving a balanced distribution of all three key components—SiO_2, Al_2O_3, and P_2O_5—with improved peak sharpness and intensity ratios.

This outcome directly aligns with the improved filtration performance observed in the experimental results. The optimized coated membrane exhibited the highest oil rejection rates and lowest residual oil concentrations across all membrane housing heights, achieving as low as 1.2 mg/L residual oil at the 4 mm housing height configuration. The enhanced membrane hydrophilicity and chemical robustness inferred from the XRD analysis are key contributors to this superior separation efficiency.

Additionally, maintaining a high degree of crystallinity ensures that the membrane remains physically stable under pressure-driven filtration conditions. This is vital for real-world industrial applications, where mechanical resilience and chemical resistance are required for long-term, sustainable performance.

In summary, Figure 7 provides final structural confirmation that the optimized nanoparticle coating strategy successfully engineered a durable, multifunctional quartz membrane system. The co-existence of SiO_2, Al_2O_3, and P_2O_5 in their crystalline forms ensures optimal synergy between oil repellence, fouling resistance, and mechanical integrity—key characteristics for advancing quartz-based membrane technologies for industrial oily wastewater treatment.

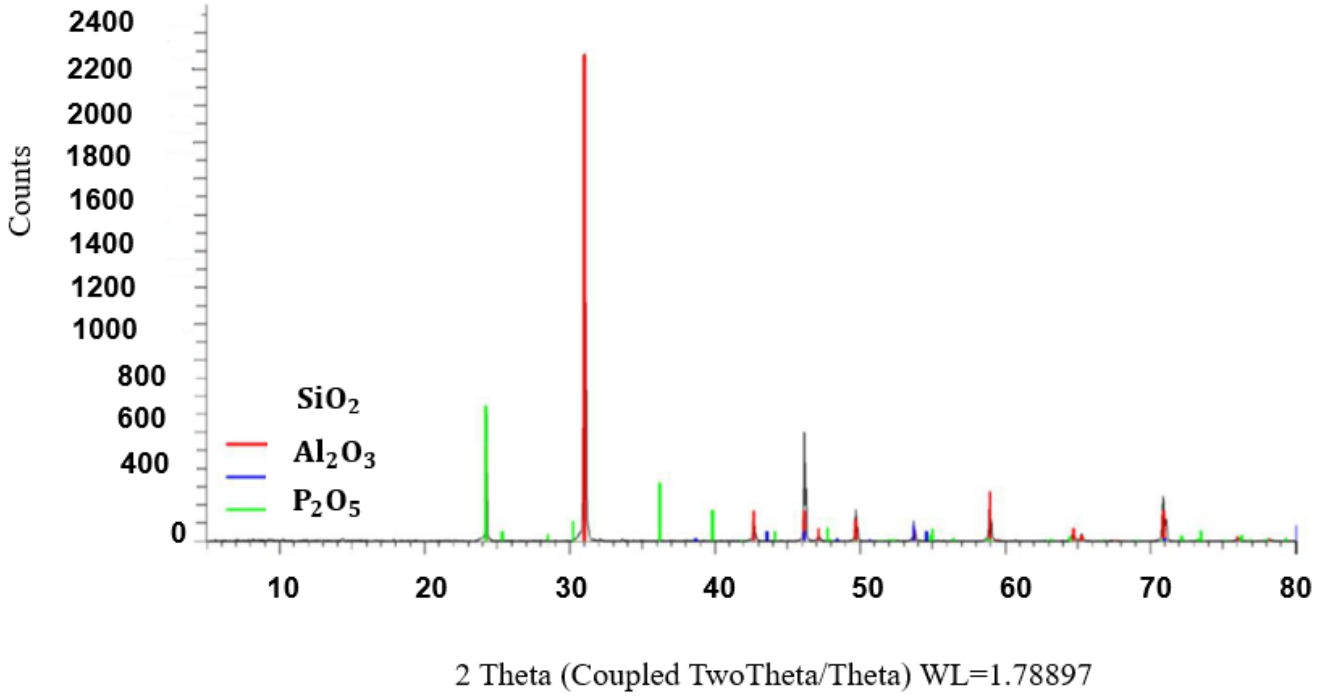

Figure 7.
XRD pattern of optimized nanoparticle-coated quartz membrane illustrating the crystalline phases of SiO_2, Al_2O_3, and P_2O_5. Sharp peaks indicate high crystallinity and confirm successful incorporation of the targeted hydrophilic nanoparticles into the quartz matrix.

3.2. Oil and Grease Concentration Analysis

Following the detailed structural and morphological characterizations by SEM and XRD, which confirmed the superior surface properties of the first nanoparticle-coated quartz membrane, oil and grease concentration analyses were conducted exclusively using this optimized material. The coated quartz membrane exhibited uniform nanoparticle distribution, enhanced hydrophilicity, and preserved crystalline integrity, making it the most suitable candidate for oil–water separation performance testing. Gravimetric oil and grease measurements were performed to assess the filtration efficacy under varying membrane housing heights. The results, summarized in Table 1, illustrate the progressive improvement in oil retention efficiency with increasing membrane height, providing critical insights into the relationship between membrane architecture and separation performance in quartz-based filtration systems.

Table 1.
Oil and grease concentration results at different membrane housing heights during quartz membrane filtration experiments.

Membrane Housing Height (mm)	Residual Oil Concentration (mg/L)	Remarks
Oil and water mixture	39567.4	Initial unfiltered synthetic oily wastewater
1	3761.5	Limited oil removal; high fouling potential
2	3635.5	Slight improvement; moderate fouling persists
3	78.5	Significant oil rejection achieved
4	1.2	Near-complete oil separation; optimal performance

3.3. Influence of Membrane Housing Height on Oil–Water Separation Performance

The impact of membrane housing height on the oil–water separation efficiency of the nanoparticle-coated quartz membranes was systematically evaluated. Figure 8 presents the relationship between membrane height and the corresponding residual oil concentration in the permeate. A clear trend is observed: increasing the membrane housing height significantly enhances oil removal efficiency, with residual oil concentrations decreasing sharply from 3761.5 mg/L at 1 mm to as low as 1.2 mg/L at 4 mm. This improvement is attributed to extended fluid–membrane interaction time and

increased packing density, which promote more effective capture of emulsified oil droplets. These findings highlight membrane housing height as a critical design parameter for optimizing filtration performance in quartz-based separation systems.

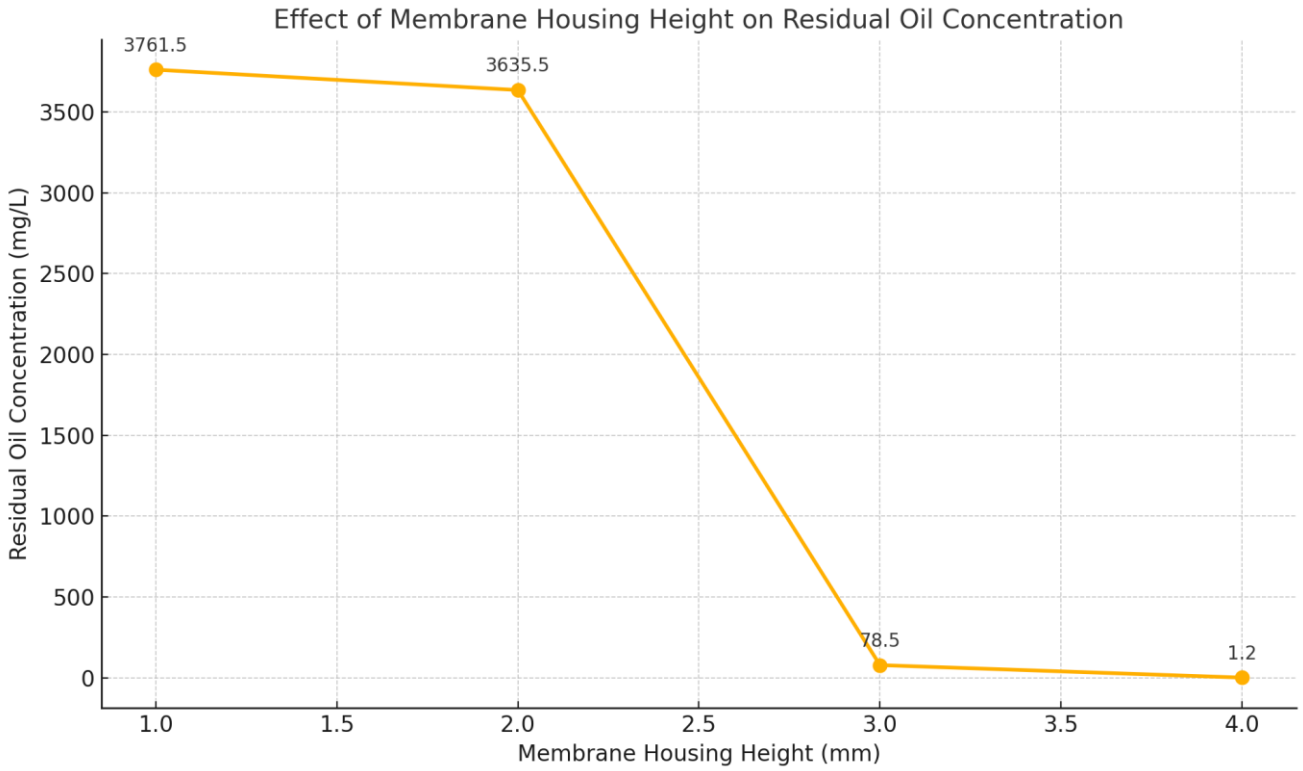

Figure 8.
Effect of membrane housing height on the residual oil concentration after filtration using nanoparticle-coated quartz membranes.

3.4. Application and Employability of Quartz for Industrial Applications

Quartz-based membranes, particularly those modified with hydrophilic nanoparticles, have emerged as promising alternatives to conventional ceramic and polymeric membranes in industrial oily wastewater treatment. Their natural abundance, mechanical resilience, and low cost make them particularly suitable for large-scale applications. The experimental results from this study—supported by SEM and XRD analyses—demonstrated that surface-engineered quartz membranes not only retain structural integrity under filtration conditions but also achieve exceptional oil rejection rates, especially at higher membrane housing heights. This positions quartz membranes as a viable, scalable solution for industries requiring robust and sustainable water separation technologies. The table below summarizes key considerations for the employability of quartz membranes in real-world industrial scenarios**.**

The data presented in Table 2 clearly illustrate that nanoparticle-coated quartz membranes possess the critical attributes required for industrial deployment in oily wastewater treatment systems. Their mechanical durability, surface stability, and high oil rejection efficiency—when paired with cost-effective material sourcing and modular scalability—offer a compelling case for their adoption in diverse industrial sectors. In particular, industries such as petrochemicals, metalworking, and automotive manufacturing stand to benefit from this technology, as it combines operational reliability with environmental compliance. Furthermore, the alignment of quartz membrane performance with sustainable development objectives, such as SDG 6 (Clean Water and Sanitation), underscores their potential to support circular water economy initiatives. Overall, the findings of this study not only validate the scientific feasibility of quartz membranes but also affirm their practical employability in real-world industrial applications.

Table 2.
Industrial Application Potential and Employability Analysis of Quartz Membranes.

Parameter	Quartz-Based Membrane (Nanoparticle-Coated)	Implications for Industrial Employability
Material Source	Naturally abundant silica (SiO_2), locally available	Cost-effective supply chain; supports circular economy strategies
Structural Integrity	Retains high crystallinity post-coating (XRD confirmed)	Suitable for long-term use under industrial pressure and chemical conditions
Surface Morphology	Uniform hydrophilic coating (SEM-validated)	Enhanced oil repellency; reduced fouling; lower maintenance frequency
Filtration Efficiency	Up to 99.9% oil rejection at 4 mm height	Meets industrial discharge standards; minimizes environmental impact
Operational Cost	Low fabrication and regeneration cost	Competitive advantage over ceramic and polymeric alternatives
Chemical Compatibility	Resistant to lubricants, hydrocarbons, acids (based on coating composition)	Applicable in petrochemical, automotive, and metalworking sectors
Scalability and Modularity	Adjustable housing height and bed volume	Easily adaptable for small-to-large scale operations
Environmental Sustainability	Promotes water reuse; no hazardous byproducts	Aligned with SDG 6 and environmental compliance requirements
Employability in Harsh Conditions	Demonstrated thermal and mechanical stability	Appropriate for high-temperature and high-pressure filtration units

4. Discussions

The results of this study provide comprehensive evidence that the combination of nanoparticle surface modification and membrane housing height optimization significantly improves the performance of quartz-based membranes for oil–water separation. The progression from raw to chemically washed and then to nanoparticle-coated quartz was essential in transforming the quartz surface from a rough, hydrophobic material to a highly hydrophilic and oil-repellent medium. SEM and EDS analyses (Figures 2–4) clearly demonstrated this surface evolution, showing increased surface smoothness, reduced contamination, and uniform nanoparticle coverage. These improvements were not merely morphological; they translated directly into enhanced functional performance, as shown by the sharp decline in residual oil concentration with increasing membrane bed height (Figure 8, Table 1).

XRD analysis further confirmed the successful integration of hydrophilic nanoparticles without compromising the quartz membrane's crystalline integrity (Figures 5–7). The retention of strong diffraction peaks associated with SiO_2, Al_2O_3, and P_2O_5 verified that the surface engineering process did not lead to amorphization or structural degradation, which is crucial for the long-term operational stability of the membrane in harsh industrial environments [30, 31]. Particularly, the presence of P_2O_5 and elemental phosphorus suggests enhanced surface charge properties that likely contribute to the high oil rejection observed [32, 33].

From a performance standpoint, the membrane housing height emerged as a critical factor. As illustrated in Figure 8, increasing the bed height from 1 mm to 4 mm resulted in a dramatic reduction in residual oil concentration from 3,761.5 mg/L to just 1.2 mg/L. This improvement is attributed to extended contact time, increased surface area, and more efficient interception of oil droplets within the membrane matrix. The trend observed is consistent with earlier studies on granular filtration systems, where deeper beds were associated with greater contaminant removal efficiency [34-36].

The novel mathematical models developed in this work provide further insights into the system's dynamics. The Height-Normalized Oil Retention Index (HNORI) and Specific Separation Capacity (SSC) confirmed that oil removal efficiency improves non-linearly with increased membrane height, validating the role of geometrical optimization in design. Meanwhile, the Dynamic Filtration Efficiency Factor (DFEF) captured the temporal fouling behavior, reinforcing the observation that the nanoparticle-coated membranes maintained performance over time with minimal flux decay. The Quartz Membrane Utilization Efficiency (QMUE) and Bed Height Effectiveness Coefficient (BHEC) offered additional tools for scaling up the technology in industrial applications, by quantifying material usage and identifying diminishing returns at higher housing configurations.

Furthermore, the oil and grease concentration results confirmed the superior efficacy of the nanoparticle-coated quartz membrane (Table 1), especially at higher membrane heights. The consistent reduction in residual oil across all stages of testing, coupled with the strong structural and morphological performance, supports the use of quartz membranes in demanding wastewater treatment environments [35]. This conclusion is further reinforced by the Application and Employability Assessment (Table 2), which outlines the cost-effectiveness, scalability, and environmental advantages of quartz as a membrane material.

Taken together, these findings demonstrate that the optimization of both membrane material (via surface engineering) and configuration (via housing height) are essential for realizing the full potential of quartz membranes in industrial oily

wastewater treatment. The synergy between morphological modification and design geometry has enabled the development of a low-cost, high-efficiency, and environmentally sustainable membrane system aligned with circular water economy principles and SDG 6 objectives. This study fills a significant gap in the literature by providing empirical evidence and predictive modeling to guide future design and application of quartz-based filtration systems in real-world scenarios.

5. Conclusion

This study demonstrated the significant role of membrane housing height and surface engineering in enhancing the performance of quartz-based membranes for oil–water separation. The integration of hydrophilic nanoparticle coatings effectively transformed raw quartz into a high-performance filtration medium, as validated through SEM and EDS analyses, which confirmed improved surface uniformity and elemental distribution. XRD analysis further affirmed the structural stability of the quartz membranes after functionalization, highlighting their suitability for industrial use.

Performance evaluation revealed that increasing the membrane housing height from 1 mm to 4 mm resulted in a dramatic reduction in residual oil concentration—from 3,761.5 mg/L to as low as 1.2 mg/L—demonstrating a direct correlation between housing height and separation efficiency. The use of novel mathematical models further reinforced these findings by providing predictive insights into oil retention dynamics, fouling behaviour, and filtration capacity.

Collectively, the results indicate that optimized quartz membranes, when appropriately configured within scalable housing designs, present a cost-effective, sustainable, and high-efficiency alternative to conventional membranes for industrial oily wastewater treatment. The system's compatibility with circular economy principles and alignment with SDG 6 goals make it a promising candidate for broad implementation in petrochemical, food processing, metalworking, and automotive industries. Building on these findings, future research will focus on long-term performance testing to evaluate membrane fouling, regeneration efficiency, and operational stability under continuous industrial flow conditions.

References

[1] T. Fan, W. Cui, Z. Yu, S. Ramakrishna, and Y.-Z. Long, "Multifunctional nanofibrous membranes for highly efficient harsh environmental air filtration and oil–water separation," *Applied Surface Science*, vol. 670, p. 160600, 2024. https://doi.org/10.1016/j.apsusc.2024.160600

[2] A. Sun *et al.*, "Design of photocatalytic self-cleaning poly (arylene ether nitrile)/nitrogen-doped Bi2O2CO3 composite membrane for emulsified oily wastewater purification," *Journal of Environmental Chemical Engineering*, vol. 11, no. 5, p. 110810, 2023. https://doi.org/10.1016/j.jece.2023.110810

[3] Z. Ren, Y. Qi, M. Zhao, B. Li, W. Jing, and X. Wei, "A composite structure pressure sensor based on quartz DETF resonator," *Sensors and Actuators A: Physical*, vol. 346, p. 113883, 2022. https://doi.org/10.1016/j.sna.2022.113883

[4] V. S. Anggraeni, P. D. Sutrisna, P. S. Goh, E. W. C. Chan, and C. W. Wong, "Development of antifouling membrane film for treatment of oil-rich industrial waste," *Materials Today: Proceedings*, 2023. https://doi.org/10.1016/j.matpr.2023.02.151

[5] Z. Feng *et al.*, "Nano graphene oxide creates a fully biobased 3D-printed membrane with high-flux and anti-fouling oil/water separation performance," *Chemical Engineering Journal*, vol. 485, p. 149603, 2024. https://doi.org/10.1016/j.cej.2024.149603

[6] N. Baig, M. Sajid, B. Salhi, and I. Abdulazeez, "Special wettable membranes for oil/water separations: A brief overview of properties, types, and recent progressa," *Colloids and Interfaces*, vol. 7, no. 1, p. 11, 2023. https://doi.org/10.3390/colloids7010011

[7] Y. Xu, X. Zeng, L. Qiu, and F. Yang, "2D nanoneedle-like ZnO/SiO2 Janus membrane with asymmetric wettability for highly efficient separation of various oil/water mixtures," *Colloids and Surfaces A: Physicochemical and Engineering Aspects*, vol. 650, p. 129352, 2022. https://doi.org/10.1016/j.colsurfa.2022.129352

[8] U. Baig *et al.*, "Insight into soft chemometric computational learning for modelling oily-wastewater separation efficiency and permeate flux of polypyrrole-decorated ceramic-polymeric membranes," *Journal of Chromatography A*, vol. 1725, p. 464897, 2024. https://doi.org/10.1016/j.chroma.2024.464897

[9] Y. Wan *et al.*, "A g-C3N4/Fe-MOF heterojunction intercalated graphene oxide membrane with persulfate activation self-cleaning property for efficient crude oil in water emulsion separation," *Journal of Membrane Science*, vol. 685, p. 121922, 2023. https://doi.org/10.1016/j.memsci.2023.121922

[10] Y. Liang *et al.*, "Oil-water separation process based on microbubble air flotation membrane device and scale-up research," *Desalination and Water Treatment*, vol. 318, p. 100312, 2024. https://doi.org/10.1016/j.dwt.2024.100312

[11] Z. Al Ansari, L. F. Vega, and L. Zou, "Emulsified oil fouling resistant cellulose acetate-MoS2-nanocomposite membrane for oily wastewater remediation," *Desalination*, vol. 575, p. 117335, 2024. https://doi.org/10.1016/j.desal.2024.117335

[12] H. Osman, E. A. Said, M. Al-Bahrani, and S. Zahmatkesh, "Effect of composite membrane flux behavior on oily wastewater treatment: Predicting and optimizing based response surface methodology and AI," *Journal of Water Process Engineering*, vol. 60, p. 105072, 2024. https://doi.org/10.1016/j.jwpe.2024.105072

[13] R. Akoumeh *et al.*, "Advances in fabrication techniques and performance optimization of polymer membranes for enhanced industrial oil-water separation: A critical review," *Journal of Environmental Chemical Engineering*, vol. 12, no. 6, p. 114411, 2024. https://doi.org/10.1016/j.jece.2024.114411

[14] X. Yang, R. Bai, X. Cao, C. Song, and D. Xu, "Modification of polyacrylonitrile (PAN) membrane with anchored long and short anionic chains for highly effective anti-fouling performance in oil/water separation," *Separation and Purification Technology*, vol. 316, p. 123769, 2023. https://doi.org/10.1016/j.seppur.2023.123769

[15] Y. Cai *et al.*, "Durable polyvinylpyrrolidone superhydrophilic modified ZIF-8 mesh membrane for gravitational oil-water separation and oil recovery," *Colloids and Surfaces A: Physicochemical and Engineering Aspects*, vol. 688, p. 133509, 2024. https://doi.org/10.1016/j.colsurfa.2024.133509

[16] Z. Dong *et al.*, "Preparation of polystyrene and silane-modified nano-silica superhydrophobic and superoleophilic three-dimensional composite fiber membranes for efficient oil absorption and oil-water separation," *Journal of Environmental Chemical Engineering*, vol. 12, no. 3, p. 112690, 2024. https://doi.org/10.1016/j.jece.2024.112690

[17] M. Purnima, T. Paul, K. Pakshirajan, and G. Pugazhenthi, "Onshore oilfield produced water treatment by hybrid microfiltration-biological process using kaolin based ceramic membrane and oleaginous Rhodococcus opacus," *Chemical Engineering Journal*, vol. 453, p. 139850, 2023. https://doi.org/10.1016/j.cej.2022.139850

[18] H. Mao *et al.*, "Piezoceramic membrane equipped with superwetting interface and in-situ ultrasound performance for efficient oil/water emulsion separation," *Desalination*, vol. 555, p. 116545, 2023. https://doi.org/10.1016/j.desal.2023.116545

[19] G. Zhu, X. Zhang, and Y. He, "Facile preparation of superhydrophilic and superoleophobic sand for efficient oil-water separation," *Journal of Water Process Engineering*, vol. 61, p. 105355, 2024. https://doi.org/10.1016/j.jwpe.2024.105355

[20] P. Grad, V. A. Hernandez, and K. Edwards, "Improved accuracy and reproducibility of spontaneous liposome leakage measurements by the use of supported lipid bilayer-modified quartz cuvettes," *Colloids and Surfaces B: Biointerfaces*, vol. 221, p. 113022, 2023. https://doi.org/10.1016/j.colsurfb.2022.113022

[21] G. Cordoyiannis, L. Bar, and P. Losada-Pérez, "Recent advances in quartz crystal microbalance with dissipation monitoring: Phase transitions as descriptors for specific lipid membrane studies," *Advances in Biomembranes and Lipid Self-Assembly*, vol. 34, pp. 107-128, 2021. https://doi.org/10.1016/bs.abl.2021.11.004

[22] Z. Bai *et al.*, "Solvent-nonsolvent regulated nano-functionalization of super-wetting membranes for sustainable oil/water separation," *Applied Surface Science*, vol. 613, p. 156085, 2023. https://doi.org/10.1016/j.apsusc.2022.156085

[23] P. D. Sutrisna, P. C. B. W. Mustika, R. P. Hadi, and Y. E. Gani, "Improved oily wastewater rejection and flux of hydrophobic PVDF membrane after polydopamine-polyethyleneimine co-deposition and modification," *South African Journal of Chemical Engineering*, vol. 44, pp. 42-50, 2023. https://doi.org/10.1016/j.sajce.2023.01.006

[24] J. Xu *et al.*, "Sustainable recycling of waste poly (vinylidene fluoride) and rational design of Janus membrane with superhydrophilic/hydrophobic asymmetric wettability for efficient separation of surfactant-stabilized water-in-oil and oil-in-water emulsions," *Colloids and Surfaces A: Physicochemical and Engineering Aspects*, vol. 684, p. 133237, 2024. https://doi.org/10.1016/j.colsurfa.2024.133237

[25] L. Cao, H. Liu, H. Li, H. Lin, and L. Li, "Dopamine co-coating with fulvic acid on PVDF membrane surface for hydrophilicity improvement and highly-efficient oily water purification," *Journal of Water Process Engineering*, vol. 64, p. 105722, 2024. https://doi.org/10.1016/j.jwpe.2024.105722

[26] S. Zhang, Y. Li, Y. Yuan, L. Jiang, H. Wu, and Y. Dong, "Biomimetic hydrophilic modification of poly (vinylidene fluoride) membrane for efficient oil-in-water emulsions separation," *Separation and Purification Technology*, vol. 329, p. 125227, 2024. https://doi.org/10.1016/j.seppur.2023.125227

[27] H. Liu *et al.*, "Construction of gradient SA-TiO2 hydrogel coated PVDF-g-IL fibre membranes with high hydrophilicity and self-cleaning for the efficient separation of oil-water emulsion and dye wastewater," *Journal of Membrane Science*, vol. 697, p. 122580, 2024. https://doi.org/10.1016/j.memsci.2024.122580

[28] J. Mulinari *et al.*, "Polydopamine-assisted one-step immobilization of lipase on α-alumina membrane for fouling control in the treatment of oily wastewater," *Chemical Engineering Journal*, vol. 459, p. 141516, 2023. https://doi.org/10.1016/j.cej.2023.141516

[29] N. Ramanamane and M. Pita, "Designing a high-performance oil–water filtration system: Surface-enhanced quartz with hydrophilic nanoparticles for sustainable water reuse and global water scarcity solutions," *Water*, vol. 17, no. 4, p. 501, 2025. https://doi.org/10.3390/w17040501

[30] P. Thiyagarajan, A. Shanmugharaj, T. Alagesan, A. Padmapriya, and R. Kalaivani, "DFT theoretical and experimental studies unraveling the structural and electronic properties of niobium doped calcium apatite ceramics," *Materials Today Communications*, vol. 35, p. 105873, 2023. https://doi.org/10.1016/j.mtcomm.2023.105873

[31] Y. Wang *et al.*, "Removal of PM and oil mist from automobile exhaust by a “hamburger” structured conjugated microporous polymers membrane," *European Polymer Journal*, vol. 195, p. 112167, 2023. https://doi.org/10.1016/j.eurpolymj.2023.112167

[32] Z. Khebli *et al.*, "Fabrication of a zircon microfiltration membrane for culture medium sterilization," *Membranes*, vol. 13, no. 4, p. 399, 2023. https://doi.org/10.3390/membranes13040399

[33] K. Fan *et al.*, "Enhanced management and antifouling performance of a novel NiFe-LDH@ MnO2/PVDF hybrid membrane for efficient oily wastewater treatment," *Journal of Environmental Management*, vol. 351, p. 119922, 2024. https://doi.org/10.1016/j.jenvman.2023.119922

[34] Z. Yin *et al.*, "Multifunctional CeO2-coated pulp/cellulose nanofibers (CNFs) membrane for wastewater treatment: Effective oil/water separation, organic contaminants photodegradation, and anti-bioadhesion activity," *Industrial Crops and Products*, vol. 197, p. 116672, 2023. https://doi.org/10.1016/j.indcrop.2023.116672

[35] H. Liu, D. Wang, H. Huang, W. Zhou, and Z. Chu, "Cysteine-based antifouling superhydrophilic membranes prepared via facile thiol-ene click chemistry for efficient oil-water separation," *Journal of Environmental Chemical Engineering*, vol. 12, no. 3, p. 112654, 2024. https://doi.org/10.1016/j.jece.2024.112654

[36] O. Samuel *et al.*, "Treatment of oily wastewater using photocatalytic membrane reactors: A critical review," *Journal of Environmental Chemical Engineering*, vol. 10, no. 6, p. 108539, 2022. https://doi.org/10.1016/j.jece.2022.108539